Imaging of Transverse Electron Transfer through a DNA Molecule by Simultaneous Scanning Tunneling and Frequency-Modulation Atomic Force Microscopy

Yasushi Maeda,[†,‡] Takuya Matsumoto,[‡,*] and Tomoji Kawai[‡]

[†]Research Institute for Ubiquitous Energy Devices, National Institute of Advanced Industrial Science and Technology (AIST), 1-8-31, Midorigaoka, Ikeda, Osaka 563-8577, Japan, and [‡]The Institute of Scientific and Industrial Research (ISIR), Osaka University, 8-1 Mihogaoka, Ibaraki, Osaka 567-0047, Japan

ABSTRACT Simultaneous scanning tunneling and frequency-modulation atomic force microscopy (STM/FM-AFM) was applied to a DNA molecule on a Cu(111) surface to analyze transverse electron transfer which is related to the electron transfer and the electrical contact in DNA-based devices. In particular, we demonstrated correlation mapping of the electron transfer parameters by visualizing specific combinations of the decay constant β and the contact conductance *G*. The results clearly revealed that electron transfer across the DNA strand varies spatially in the DNA molecule. This spatial variation is probably correlated with deformation of DNA on the surface. From quantitative analysis, the decay constant β was estimated to be 3.3 nm^{-1}, which is consistent with previously reported values for π-conjugated molecules.

KEYWORDS: scanning tunneling microscopy · frequency-modulation atomic force microscopy · DNA · electron transfer · decay constant

Molecular-based self-assembly techniques have been attracting considerable interest for fabricating molecular devices. DNA is a suitable molecule for these techniques because programmable self-assembly enables it to be used to fabricate designed nanostructures.[1−5] For example, Rothemund fabricated nanosized smiley faces and maps of the American continent using the DNA scaffolding technique.[6] When DNA-based methods are used to produce devices, the electrical properties of DNA strongly influence device performance.

Scanning tunneling microscopy (STM) is a powerful tool for investigating electrical properties of organic molecules on a substrate.[7] Bumm *et al.* used STM to investigate the electron transfer through alkanethiol films on a gold substrate, and they estimated the decay constant β to be 11 nm^{-1}, which agrees well with values obtained by other methods.[8] In their method, β was estimated by comparing the constant-current STM topography with the known molecular height. Unlike alkanethiol films, DNA does not form a well-defined adsorption structure on a substrate; consequently, it is necessary to measure the height of DNA as well as the STM topography. To settle this problem, we employed simultaneous STM and frequency-modulation atomic force microscopy (STM/FM-AFM). Recent progress in FM-AFM has resulted in atomic resolution being achieved in STM/FM-AFM, and the correlation between the tunneling current and the force was investigated in detail on clean, well-defined surfaces.[9−14]

In the present study, we applied STM/FM-AFM to analyze transverse electron transfer through a DNA molecule laid on a Cu(111) surface: the transverse electron transfer should play an important role in the device with a specific configuration, such as metal particles assembled on DNA template laid on a metal surface. Herein, we visualized the electron transfer parameters (*i.e.*, the decay constant β and the contact conductance *G*) and we find that the transverse electron transfer varies spatially in a DNA molecule. From quantitative analysis, we estimated the decay constant β across a DNA strand to be 3.3 nm^{-1}, which is consistent with previously reported values for π-conjugated molecules.

RESULTS AND DISCUSSION

Figure 1 panels a−c show (left) STM and (center) frequency-shift images and (right) line profiles of DNA molecules, Cu monatomic steps, and aggregates of buffer molecules observed by STM/FM-AFM, respectively. Two DNA molecules twisted around

* Address correspondence to matsumoto@sanken.osaka-u.ac.jp.

Received for review January 24, 2011 and accepted March 23, 2011.

Published online March 23, 2011
10.1021/nn200291f

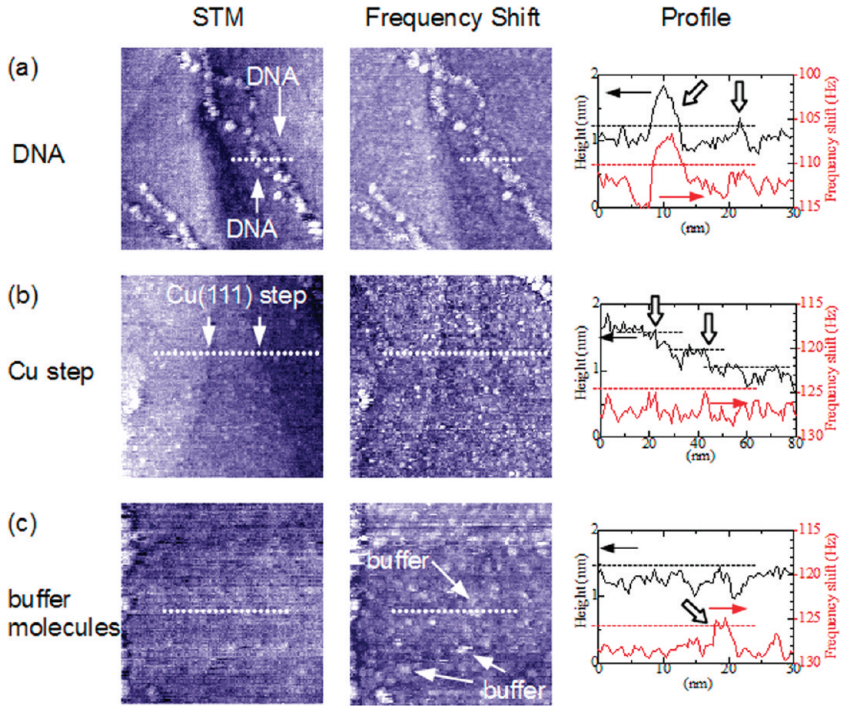

Figure 1. Simultaneously obtained (left) STM and (center) frequency-shift images and (right) line profiles of (a) DNA molecules, (b) Cu monatomic steps, and (c) aggregates of buffer molecules on a Cu(111) surface. The white arrows in the images correspond to those in the line profiles. The sample bias voltage was 3 V and the average tunneling current was 10 pA. (a) Double-stranded DNA molecules are observed in both the STM and frequency-shift images. (b) Upper and lower terraces across Cu steps show the same contrast in the frequency-shift image. (c) Aggregates of buffer molecules are observed only in the frequency-shift image.

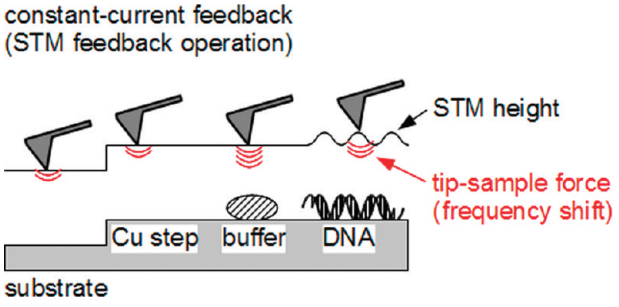

Figure 2. A schematic illustration of STM/FM-AFM observation of a Cu step, an aggregate of buffer molecules, and a DNA molecule under a constant-current STM feedback condition. In the STM image, the STM height reflects the Cu step. In contrast, the buffer molecules appear almost transparent since it is insulating. For DNA, both STM height and frequency shift are influenced by the presence of the DNA molecule.

each other are visible in Figure 1a. Protrusions are observed in the DNA molecules at an interval of 3−5 nm, which is consistent with the pitch length of B-form DNA. This implies that our STM/FM-AFM system has a sufficiently high spatial resolution. The DNA molecules are observed in both the STM and the frequency-shift images (Figure 1a). In contrast, upper and lower terraces across the Cu steps show the same contrast in the frequency shift image (Figure 1b) and many particles (assumed to be aggregates of Tris-HCl and/or EDTA molecules in the buffer solution) are observed in only the frequency-shift image (Figure 1c). These differences are schematically illustrated in Figure 2. The frequency shift is constant for conductive objects (such as the Cu steps) because the tip−sample distance is kept constant during scans. Insulating molecules (such as the aggregates of buffer molecules) appear transparent in STM images. Thus, reducing the tip−sample distance alters the frequency shift. In the case of DNA, both the STM height and frequency shift are modified by the presence of the DNA molecule, implying that DNA has a measurable conductivity.

For a more quantitative analysis of the correlation between the STM height (H_{STM}) and the frequency shift (Δf), the local displacement of H_{STM} and Δf against the surface are plotted in Figure 3 ($H_{STM}-\Delta f$ plot). As Figure 3 shows, the data points for the Cu steps and

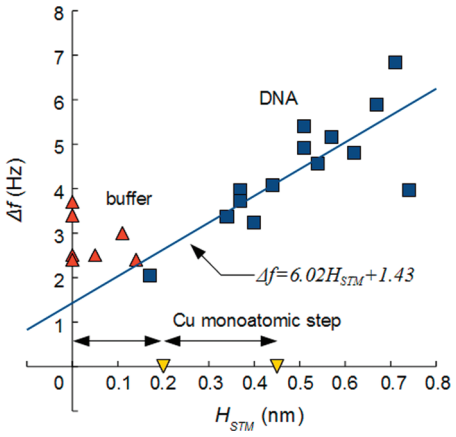

Figure 3. Plot of frequency shift as a function of STM height ($H_{STM}-\Delta f$ plot). The squares, inverted triangles, and triangles correspond to DNA, Cu steps, and buffer molecules, respectively. The data points for Cu steps and buffer molecules are located on or near the horizontal and vertical axes, respectively. The Cu step heights are consistent with the monatomic step height of Cu(111) (0.208 nm). The data points for DNA are widely distributed, and the frequency shift increases linearly with the STM height. The plots are fitted with the straight line $\Delta f = 6.02H_{STM} + 1.43$.

the buffer molecules are located on or near the horizontal and vertical axes, respectively. In addition, the step heights (average value of 0.23 nm) are consistent with the monatomic step height of Cu(111) (0.208 nm). The data points for DNA are widely distributed (with heights from 0.17 to 0.74 nm) and the frequency shift increases linearly with the STM height. Since the average STM height (0.61 nm) is smaller than the average AFM height (0.76 nm) obtained by constant-amplitude AFM, the tip−sample distance on DNA molecules is probably less than that on the substrate in this STM/FM-AFM observation. This is consistent with the increase in the frequency shift when the tip−sample distance is reduced in the tunneling region observed by Guggisberg *et al.* for dynamic lever STM.[15]

Electron Transfer in STM/FM-AFM. We analyzed the electron transfer of DNA using the following procedure. According to Bumm *et al.*, the correlation between the STM height (H_{STM}) and the height of a molecule (H_{mol}) is expressed by

$$H_{STM} = \left(1 - \frac{\beta}{22}\right) H_{mol} + \frac{1}{22}\ln(G) \qquad (1)$$

where β (nm^{-1}) is the decay constant and G is the contact conductance (see Supporting Information). Here, we assume that the frequency shift is proportional to the mth power of the tip−sample distance. If $H_{mol} - H_{STM}$ is sufficiently small, the relative frequency shift is given by $\Delta f = AmL_0^{-m-1}(H_{mol} - H_{STM})$, where L_0 is the tip−sample distance on the substrate and A is a constant. Eliminating H_{mol} from eq 1, we obtain the following expression between Δf and H_{STM}

$$\Delta f = \frac{B}{22 - \beta}\{\beta H_{STM} - \ln(G)\} \qquad (2)$$

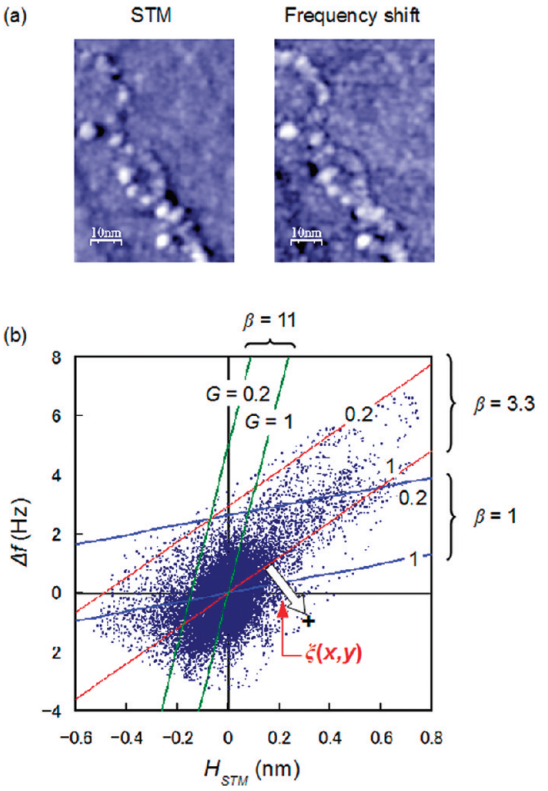

Figure 4. (a) Simultaneously obtained (left) STM and (right) frequency-shift images of DNA molecules. (b) A plot of frequency shift as a function of STM height ($H_{STM}-\Delta f$ plot) obtained from the images. H_{STM} and Δf of each pixel point (x, y) in the images are plotted as a data point in graph b. The distance $\xi(x, y)$ from a data point to a straight line is measured for each point to obtain a correlation map of the electron transfer parameters (β, G). Straight lines correspond to various combinations of (β, G).

where $B = AmL_0^{-m-1}$. As the $H_{STM}-\Delta f$ plot for DNA shows (see Figure 3), Δf increases linearly with H_{STM}. This indicates that eq 2 is suitable for analyzing DNA molecules. The $H_{STM}-\Delta f$ plot is fitted with a straight line ($\Delta f = sH_{STM} + t$) and comparing this equation with eq 2 gives

$$\frac{\ln(G)}{\beta} = -\frac{t}{s} \qquad (3)$$

From Figure 3, the slope s and the intercept t for DNA molecules are determined to be 6.02 and 1.43, respectively. To estimate β and G, the average STM (0.61 nm) and AFM (0.76 nm) heights for DNA obtained by STM/FM-AFM and AFM, respectively, are used for H_{STM} and H_{mol} in eq 1. Substituting these values into eqs 1 and 3, we estimate the β and G of DNA to be 3.3 nm^{-1} and 0.45, respectively. According to Bumm's theory, these values should lie in the ranges $0 < \beta < 22$ and $0 < G < 1$. The obtained values lie within these ranges. Values of β of 11 and 3.5−5 nm^{-1} have been previously reported for alkyl chains and π-conjugated systems, respectively.[16] Our β value is close to the latter, which is consistent with the fact that the DNA molecule contains π-conjugated systems.

Correlation Mapping of Electron Transfer Parameters. As Figure 3 shows, the data points for DNA deviate slightly

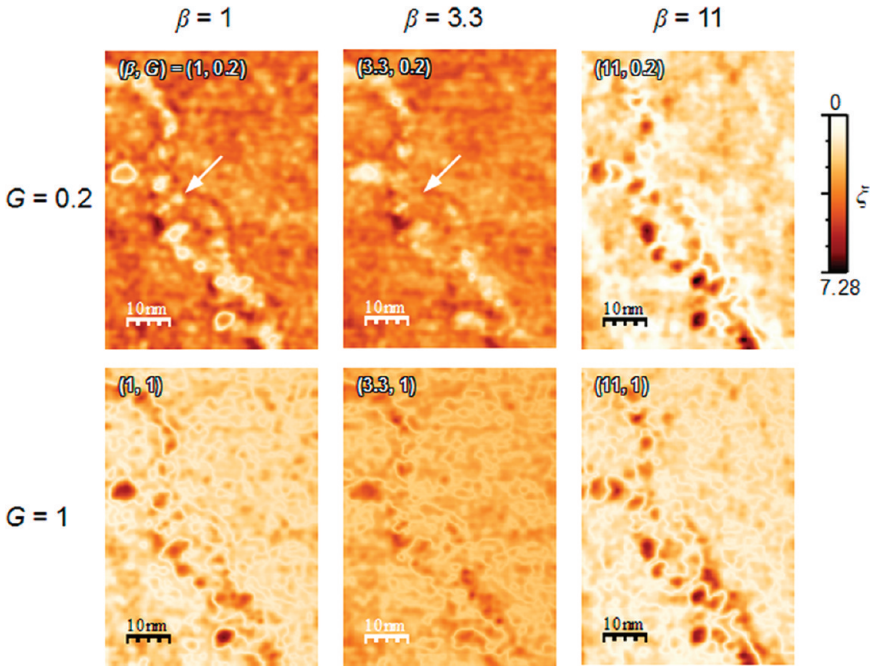

Figure 5. Correlation maps of electron transfer parameters (β, G) obtained from the STM and frequency-shift images in Figure 4a. In the images, white regions correspond to the specific (β, G) represented in each image. DNA molecules appear light at (β, G) = (3.3, 0.2) and (1, 0.2). (β, G) varies spatially in DNA molecules. For example, although a large area of the DNA molecules is observed at (3.3, 0.2), the arrowed position is observed at (1, 0.2).

from a straight line, suggesting that the transverse electron transfer varies spatially in the molecule. Two-dimensional analysis is preferable for revealing the spatial variation. This section presents correlation maps of electron transfer parameters, in which the spatial distribution of specific combinations of electron transfer parameters (β, G) is visualized in the following manner (see Figure 4). First, the STM height (H_{STM}) and the frequency shift (Δf) of each pixel point (x, y) in the simultaneously obtained STM and frequency-shift images are plotted in $H_{STM}-\Delta f$ space; for example, Figure 4b is obtained from the images in Figure 4a. Next, the perpendicular distance $\xi(x, y)$ from a data point to a straight line is measured for each point. $\xi(x, y)$ indicates the correlation between the images and the specific (β, G); $\xi(x, y) = 0$ implies that (β, G) at the pixel point (x, y) is equal to the specific (β, G). Consequently, colored mapping of $\xi(x, y)$ generates a correlation map of the electron transfer parameters (β, G).[17]

Figure 5 shows the correlation maps obtained from Figure 4a. In the images, white regions correspond to $\xi(x, y) = 0$. When $G = 1$, which is the value for the substrate, the Cu substrate appears white regardless of the value of β. For a lower G value ($G = 0.2$), the color of DNA depends on β. DNA molecules appear dark for $\beta = 11$, whereas they appear light for $\beta \leq 3.3$. These results are qualitatively consistent with the results in the previous section. Note that, $G = 0.2$ is slightly smaller than the estimated value of 0.45 because the correlation mapping is influenced by image processing procedures (*e.g.*, plane fitting). The value of β varies spatially in the DNA molecule in the correlation maps. For example, a large area of the DNA molecules appears light with $\beta = 3.3$, whereas the position indicated by the arrows in Figure 5 has a lower β of 1. This variation is possibly due to changes in the local electronic structure induced by the deformation of the DNA molecule on the surface.

CONCLUSIONS

To investigate the transverse electron transfer of DNA/Cu(111), correlation mapping of electron transfer parameters (β, G) was performed using STM/FM-AFM. In the images, the decay constant β varied in the DNA molecule, indicating that our method can be used to analyze the two-dimensional distribution of transverse electron transfer on a nanometer scale. Hence, we consider that this method is useful for revealing the conductivity properties of DNA-based devices.

METHODS

All experiments were performed using a homemade ultra-high vacuum scanning probe microscopy (SPM) system equipped with a SPM head (JEOL). The base pressure of the system was of the order of 10^{-8} Pa. The substrate used was a Cu(111) thin film prepared by thermal evaporation on a freshly cleaved mica surface. Circular double-stranded DNA (pBlue-Script II KS(-), Stratagene, 2961 base pairs) was deposited on the

surface by pulse injection. The experimental details have been reported elsewhere.[18,19]

STM/FM-AFM performed using a rectangular conductive cantilever (silicon-MDT) with a spring constant of 14 N/m and a resonance frequency of 300 kHz. The cantilever was made of highly boron-doped Si (specific resistance: 0.002 Ω·cm). In our STM/FM-AFM system, the cantilever deflection was detected by deflection of an optical beam and the oscillation amplitude and frequency shift were detected using an additional two-phase lock-in amplifier and a home-built crystal-controlled heterodyne phase-locked loop circuit, respectively. The time-averaged tunneling current was detected through a STM preamplifier with the conductive cantilever oscillated in self-oscillation mode with constant excitation. A frequency-shift image was simultaneously obtained with a STM topography by controlling the tip−sample distance using the time-averaged tunneling current. Prior to STM/FM-AFM measurements, the tip was sharpened by contacting the surface with a load of 0.1−1.0 μN and then applying a high voltage (typically ±10 V) between the tip and the substrate. The sample bias voltage and the tunneling current were set to +3 V and 10 pA, respectively. The obtained frequency shift was typically in the range of −100 to −200 Hz, and typical free oscillation amplitude was roughly estimated to be 160 nm. We performed AFM observations with the same setup to measure the height of a DNA molecule. It was operated in constant-amplitude mode with no bias voltage. The oscillation amplitude was set to 90% of the free oscillation amplitude. The obtained images were processed by using WSxM software.[20]

Supporting Information Available: Derivation of the correlation between H_{STM} and H_{mol} (eq 1). This material is available free of charge *via* the Internet at http://pubs.acs.org.

REFERENCES AND NOTES

1. LaBean, T. H.; Li, H. Constructing Novel Materials with DNA. *Nanotoday* **2006,** *2*, 26–35.
2. Li, H.; Carter, J. D.; LaBean, T. H. Nanofabrication by DNA Self-Assembly. *Mater. Today* **2009,** *12*, 24–32.
3. Maeda, Y.; Nakamura, T.; Uchimura, K.; Matsumoto, T.; Tabata, H.; Kawai, T. Controlled Conjugation of Nanoparticles with Single Stranded DNA. *J. Vac. Sci. Technol., B* **1999,** *17*, 494–496.
4. Maeda, Y.; Tabata, H.; Kawai, T. Two-Dimensional Assembly of Gold Nanoparticles with a DNA Network Template. *Appl. Phys. Lett.* **2001,** *79*, 1181–1183.
5. Maeda, Y.; Maeda, Y. Y.; Okada, T.; Kodaka, M.; Fujitani, T.; Tsubota, S. Site-Selective Deposition of Au Nanoparticles on Au Islands on Highly Oriented Pyrolytic Graphite Substrate Using DNA-Based Method. *Jpn. J. Appl. Phys.* **2005,** *44*, 5400–5402.
6. Rothemund, P. W. Folding DNA to Create Nanoscale Shapes and Patterns. *Nature* **2006,** *440*, 297–302.
7. Tanaka, H.; Kawai, T. Partial Sequencing of a Single DNA Molecule with a Scanning Tunneling Microscope. *Nat. Nanotechnol.* **2009,** *4*, 518–522.
8. Bumm, L. A.; Arnold, J. J.; Dunbar, T. D.; Allara, D. L.; Weiss, P. S. Electron Transfer through Organic Molecules. *J. Phys. Chem. B* **1999,** *103*, 8122–8127.
9. Güthner, P. Simultaneous Imaging of Si(111) 7 × 7 with Atomic Resolution in Scanning Tunneling Microscopy, Atomic Force Microscopy, and Atomic Force Microscopy Noncontact Mode. *J. Vac. Sci. Technol. B* **1996,** *14*, 2428–2431.
10. Ashino, M.; Sugawara, Y.; Morita, S.; Ishikawa, M. Atomic Resolution Noncontact Atomic Force and Scanning Tunneling Microscopy of TiO_2(110)-(1 × 1) and (1 × 2): Simultaneous Imaging of Surface Structures and Electronic States. *Phys. Rev. Lett.* **2001,** *86*, 4334–4337.
11. Loppacher, Ch.; Bammerlin, M.; Guggisberg, M.; Schär, S.; Bennewitz, R.; Baratoff, A.; Meyer, E.; Güntherodt, H.-J. Dynamic Force Microscopy of Copper Surfaces: Atomic Resolution and Distance Dependence of Tip−Sample Interaction and Tunneling Current. *Phys. Rev. B* **2000,** *62*, 16944–16949.
12. Arai1, T.; Tomitori, M. Electric Conductance through Chemical Bonding States being Formed between a Si Tip and a Si(111)-(7 × 7) Surface by Bias−Voltage Noncontact Atomic Force Spectroscopy. *Phys. Rev. B* **2006,** *73*, 73307.
13. Özer, H. Ö.; O'Brien, S. J.; Pethica, J. B. Local Force Gradients on Si(111) during Simultaneous Scanning Tunneling/Atomic Force Microscopy. *Appl. Phys. Lett.* **2007,** *90*, 133110.
14. Sawada, D.; Sugimoto, Y.; Morita, K.; Abe, M.; Morita, S. Simultaneous Measurement of Force and Tunneling Current at Room Temperature. *Appl. Phys. Lett.* **2009,** *94*, 173117.
15. Guggisberg, M.; Bammerlin, M.; Lüthi, R.; Loppacher, Ch.; Battiston, F.; Lü, J.; Baratoff, A.; Meyer, E.; Güntherodt, H.-J. Comparison of Dynamic Lever STM and Noncontact AFM. *Appl. Phys. A: Mater. Sci. Process.* **1998,** *66*, S245–S248.
16. Ishida, T.; Mizutani, W.; Aya, Y.; Ogiso, H.; Sasaki, S.; Tokumoto, H. Electrical Conduction of Conjugated Molecular SAMs Studied by Conductive Atomic Force Microscopy. *J. Phys. Chem. B* **2002,** *106*, 5586–5892.
17. Strictly, the values of (β, G) cannot be determined uniquely because they are defined only by equation 3. For a better understanding, the values shown in Figures 4 and 5 are calculated by the same procedure described in the section "Electron transfer in STM/FM-AFM".
18. Maeda, Y.; Matsumoto, T.; Kawai, T. Observation of Single- and Double-Stranded DNA using Noncontact Atomic Force Microscopy. *Appl. Surf. Sci.* **1999,** *140*, 400.
19. Maeda, Y.; Matsumoto, T.; Tanaka, H.; Kawai, T. Imaging of the DNA (Deoxyribonucleic Acid) Double Helix Structure by Noncontact Atomic Force Microscopy. *Jpn. J. Appl. Phys.* **1999,** *38*, L1211.
20. Horcas, I.; Fernandez, R.; Gomez-Rodriguez, J. M.; Colchero, J.; Gomez-Herrero, J.; Baro, A. M. WSXM: A Software for Scanning Probe Microscopy and a Tool for Nanotechnology. *Rev. Sci. Instrum.* **2007,** *78*, 013705.